International Journal of Physical Sciences Vol. 7(11), pp. 1762 - 1772, 9 March, 2012
Available online at http://www.academicjournals.org/IJPS
DOI: 10.5897/IJPS11.1800
ISSN 1992 - 1950 ©2012 Academic Journals

Full Length Research Paper

Micro and nano thermal flow characteristics of a flat plate heat pipe heat spreader

In Seon Yu, Seok Ho Rhi* and Kyoung Il Cha

School of Mechanical Engineering, Department of Electrical Engineering, Chungbuk National University, 410 Sung-Bong Ro, HeungDuk-Gu, Cheong-Ju, Chungbuk, Korea.

Accepted 09 February, 2012

The present study investigates the characteristics and heat transfer performance of a flat heat pipe (FHP) heat spreader with various wick structures. A flat heat pipe heat spreader exemplifies successful heat transfer applications for highly efficient devices in space, energy technology, electronics cooling etc. The present experimental and simulation results reveal the heat transfer characteristics of a flat heat pipe with various parameters in the range of 5~20W. In the experimental study, eight different wick structures were evaluated in order to find the optimum wick, and various working fluids such as water, acetone, ethanol, and TiO_2-nanofluids were used since the main driving force comes from the capillary force generated in the wick. The 0.1%-TiO_2 nanofluidic flat heat pipe system exhibited the best heat spreading performance. In the present study, a simulation based on the thermal resistance network with special modified spreading resistance was conducted. The simulation results show a reasonable agreement with the experimental results.

Key words: Heat pipe, heat transfer, heat spreader, thermal management, nanofluid.

INTRODUCTION

Recently, heat pipes which are heat transfer devices that are easy to constitute in smaller volumes, thinner thicknesses, simple shapes, and larger cooling capacities are widely used to cool electric and electronic components. Also, a heat pipe is an important component found in various smart computing systems.

A flat heat pipe is a heat pipe which has a rectangular plate type and a very thin cross section, unlike existing heat pipe models that have a kind of circular cross section. A flat heat pipe (FHP) has been called as a flat type vapor camber in the electronics cooling field. Flat heat pipes are commonly used in electronic products such as a small space or thin notebooks that cannot contain circular heat pipes because of their size (Lee et al., 2002; Kim et al., 2003).

The flat heat pipe heat spreader used in this study consists of an evaporator, wick structure which acts as a passage for liquid state working fluid, a container and internal working fluid. The operating principle of the flat heat pipe is described in Figure 1(a) and shows that, if heat is applied to the device's heater, the column in the upper side is passed to the wick structure through the heater casing. The liquid state working fluid filling the wick structure is evaporated by absorbing the heat, and the steam vapor is spread through the passage formed in the wick, as presented in Figure 1(a).

Hui and Tan (1994) derived a relational formula applying numerical models for the temperature distribution of the thermal diffusion between flat heat pipes and copper heat sinks using the changes in the heat transfer coefficient according to heat source size, thickness of the flat heat pipe, and the heat source and heat sink material. Song et al. (1994) deduced numerical equations for the average and maximum thermal constriction/spreading resistances in the flat plate with a larger area than the heat source. Oh et al. (2001) reported that a shorter length increases the heat transfer performance of a small heat pipe with a copper based mesh wick structure. Avenas et al. (2002) evaluated the thermal performance of a flat heat pipe, and found that 40% of the thermal resistance of the heat pipe is reduced

*Corresponding author. E-mail: rhi@chungbuk.ac.kr. Tel: +82-432612444, +82-1044377575. Fax: +82-432632441.

by using pure copper as a wick structure.

Kalahasti and Yogendra et al. (2002) compared and analyzed the research on the experimental and numerically analyzed methods of micro heat pipes. Kang and Tsai et al. (2004) manufactured three different types of machining grooves which were 20 μm at the evaporator, adiabatic section, condenser section, and used 100 mesh copper screen wick, and results were obtained up to 35 W with a heat source temperature of 57.78°C. Go and Kim (2004) revealed the possibility of heat pipe thermal diffusion for low cost devices by developing a heat pipe with dimensions of 83 × 69 mm, a thickness of 1.67 mm and a rectangular structure with a micro-wick structure using metal etching technology.

Kwark (2005) presents experimental research of a simple thermosyphonic liquid heat spreader fabricated using thin copper blocks and copper tubes saturated with water at 2.29 psia. It exhibited remarkable thermal performance by dissipating heat flux of 119 W/cm^2 with below 100°C chip temperature as a typical condition.

Thomas et al. (2005) present a heat spreader to cool a microprocessor with micro channel heat pipe that can capture and transfer heat flux in excess of 200 W/cm^2. Wang (2011) investigated the performance of a vapor chamber (10 cm × 8.9 cm with a 2.1 cm × 2.1 cm or a 1.1 cm × 1.1 cm heating area), in which parallel grooves were made on the inner surface of the top plate with inter-groove openings, while the inner surface of the bottom plate was sintered. In their study, the vapor chamber resistances were measured for an increasing heat load from 80 W to beyond 300 W.

Yasushi et al. (2006), Hsieh et al. (2007) and Gerardo et al. (2008) reported the simulation results for a flat heat pipe type heat spreader. Yahushi et al. (2006) suggested a mathematical model to simulate a vapor chamber to cool the new generation of electronics. The center heated vapor chamber was studied mathematically and experimentally and the compared results showed close agreement. Hsieh et al. (2007) adopted a three-dimensional simulation method to analyze the thermal resistance of a cubic vapor chamber thermal spreader with a constant heat flux over the projected heating surface. Gerardo et al. (2008) gave the simulation results on the stability of a transient computational analysis of the vapor core in large flat plate heat pipe heat spreaders. Their investigations were performed using various combinations of time step size and relaxation parameters, to obtain a stable, converged result. Typical distributions of the field variables in the vapor core of the type of large flat plate heat pipes analyzed were also presented and discussed.

Wang (2011) reports on the theoretical, simulation and experimental studies of a light emitting diode (LED) vapor chamber using the illumination-analysis method to investigate the thermal performance of three kinds of LED based plates. His results show that the thermal performance of the LED vapor chamber-based plate is better than that of the LED copper-based plate with an input power above 5 W. However, the wick structure of the vapor chamber is not finely defined, which is the main driving force.

Wong et al. (2012) studied the evaporation process in the wick of an operating flat plate heat pipe with a sintered two-layer 100 + 200 mesh copper wick (0.26 mm thick) and three different working fluids such as deionized water, methanol and acetone. Their results indicate that the maximum heat loads for water are far greater than those of methanol and acetone.

A nanofluid that is used in the present FHP system is a TiO_2-nano particle suspension in a conventional host fluid which enhances the thermal and heat transporting characteristics of the conventional fluid (Choi, 1995; Das et al., 2003). Most of the investigations of a heat pipe with nanofluids have been carried out experimentally with indefinite results such as reduction of thermal resistance, enhanced critical heat flux, particle deposition and particle aggregation etc. (Chien et al., 2003; Tsai et al., 2004; Kang, 2006; Ma et al., 2006; Lim et al., 2010; Han et al., 2011). Maryam et al. (2010) established analytical models to study the effect of using a nanofluid within flat-shaped heat pipes. They established the existence of an optimum nanoparticle concentration level and wick thickness to maximize the heat removal capability of a flat-shaped heat pipe.

The purpose of this research is to pioneer and apply a new application of nanofluids and various wick structures. A novel idea applied to the heat pipe heat spreader is to suspend nano-metal particles in the base fluid to improve the fluid's thermal properties. In the present study, the flat heat pipe's heat transfer and diffusion performance in accordance with the wick structure and working fluid were analyzed to evaluate the various effects.

Analysis (thermal resistance analogy)

The simulation with a thermal resistance network model of the flat heat pipe can predict various performance parameters and the temperature distribution from the heat source to the sink with one-dimensional analysis.

By default, the simulation method in this study was performed by the thermal resistance network model. The thermal resistance model described in Figure 1(a) shows that the thermal resistance model must be determined through the various two phase flow parameters involved. Initially, the working fluid of a FHP obtains the heat at the bottom surface of the evaporator section. As the fluid progresses along the evaporator section and the heat spreads to the side edges, the vapor fraction increases and hence the apparent flow velocity increases. Two-phase forced convection becomes dominant in a thin micro flat space. The simulation estimates the temperatures along the flow passage of the FHP. The entire simulation of the thermal resistance model is

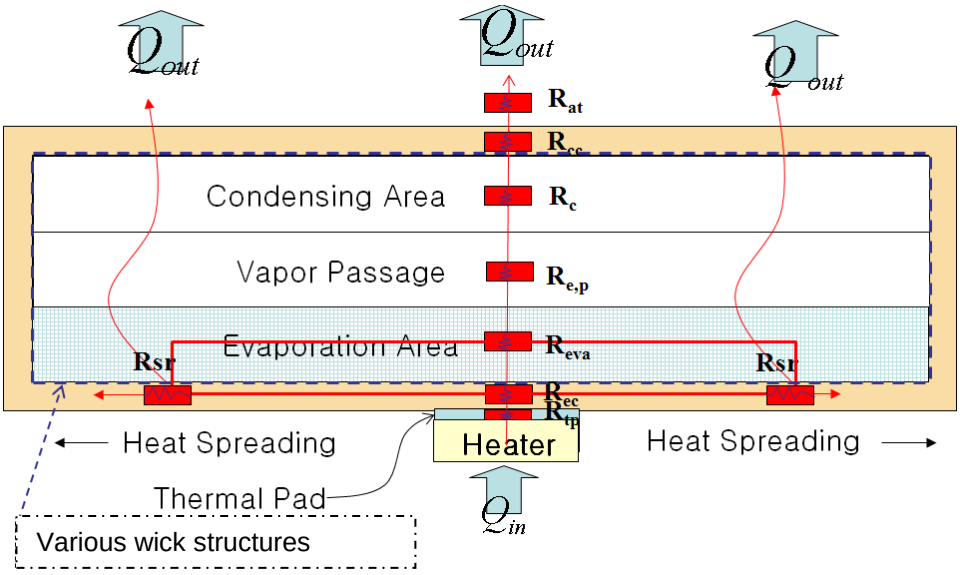

(a)

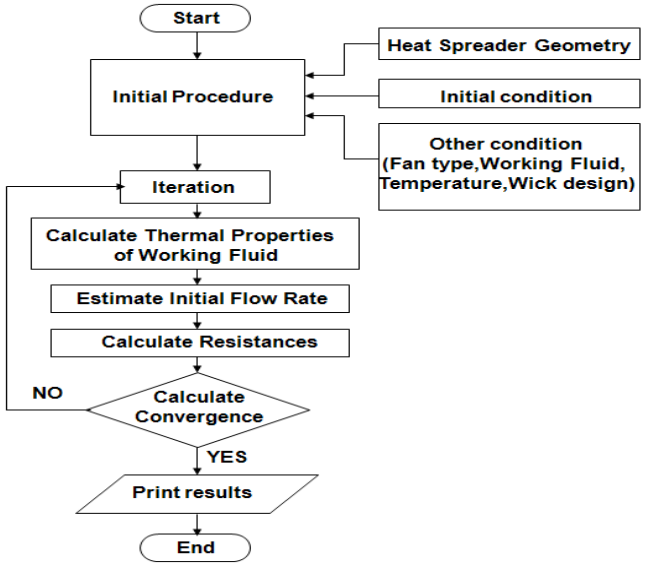

(b)

Figure 1. FHP simulation model and procedure; (a) Flat heat pipe heat spreader model (b) simulation logic.

shown in the flow charts in Figure 1(b).

The calculation of the system's thermal performance can be expressed by the simple physical Equation 1.

$$Q = \frac{T_h - T_c}{\sum R} \quad (1)$$

As follows, each thermal resistance used to analyze the system is: thermal resistance of the thermal pad

$$R_{tp} = \frac{\delta_{tp}}{k_{tp} A_{tp}} \quad (2)$$

Thermal resistance of the case in the evaporator section:

$$R_{ec} = \frac{\delta_{case}}{k_{case} A_{rh}} \quad (3)$$

Spreading thermal resistance (Song, 1994):

$$\phi_c = \frac{\tanh(\lambda \times \tau) + \frac{\lambda}{Bi}}{1 + \frac{\lambda}{Bi}\tanh(\lambda \times \tau)} \quad (4)$$

$$\psi = C\left(\frac{\varepsilon\tau}{\sqrt{\pi}} + \frac{1}{\sqrt{\pi}}(1-\varepsilon)\cdot\phi_c\right) \quad (5)$$

$$R_{sr} = \frac{\psi}{\sqrt{\pi}k_c\sqrt{\frac{A_s}{\pi}}} \quad (6)$$

In this study, Song's modified equation is suggested to identify the current experimental results with empirical constant, *C*. Where, *C* is a constant obtained from experimental results, the value of *C* = 10.0 was estimated and used in the simulation. Evaporation thermal resistance:

$$R_{eva} = \frac{1}{h_e A_{cr}} \quad (7)$$

Thermal resistance from the evaporator's vapor passage by Clapeyron equation (Chi, 1976):

$$R_{e,p} = \frac{T_v(P_{v,e} - P_{v,c})}{Q\rho_v h_{fg}} \quad (8)$$

Condensation thermal resistance:

$$R_c = \frac{1}{h_c A_{cr}} \quad (9)$$

Thermal resistance of the case in the condenser section:

$$R_{cc} = \frac{\delta_{case}}{k_{case}A_{case}} \quad (10)$$

Air convective thermal resistance:

$$R_{at} = \frac{1}{h_{at}A_c} \quad (11)$$

Verifying the empirical correlations of the nucleate boiling heat transfer coefficient was necessary to model the internal evaporative heat transfer phenomena of a flat heat pipe. Among them, Savchenkov and Gorbis (1976)'s interaction equation was analyzed, and was found to be similar when the experimental data and calculation were verified with it.

Savchenkov and Gorbis (1976):

$$h_e = \frac{3.43k_l\,\mathrm{Re}^{0.09}}{L_b}\left(\frac{\rho_l}{\rho_v}\right)^{0.21}\left(D\sqrt{g\frac{(\rho_l-\rho_v)}{\sigma}}\right)^{0.81} \quad (12)$$

$$L_b = \sqrt{\frac{\sigma}{g(\rho_l - \rho_v)}}$$

To identify condensation thermal resistance, the results analyzed by Nusselt's film condensation theory (Holman, 1996) are close to the experimental data (Lee et al., 2002). Nusselt (Holman, 1996):

$$h_c = \pi^{1/3}(4/3^{4/3})\left[\frac{\rho_l(\rho_l-\rho_v)g\sin\phi h_{fg}k_l^3 D}{\mu_l Q_c}\right]^{1/3} \quad (13)$$

EXPERIMENTALS

As shown in Figure 2(a) and (c), to evaluate the heat transfer performance of the flat heat pipe with various types of micro wicks, an experimental system with a variety of easily replaceable wick structures was designed, and conducted to find the optimum wick structure for a flat heat pipe. A simple connectable and bolt jointed evaporation and condensation section was designed to enable a comprehensive experimental study with various wicks.

As described in Figure 2(b), at the top of the FHP, a copper case, wick, and silicone pad were assembled in that order. The bolts at the top of the condenser section case were fixed by Teflon and copper plate to tightly connect the top and bottom plate. The empty wick space was manufactured to install various wick structures [150 × 100 (mm)]. The thickness of the bottom plate (evaporation part) and the top plate (condensation part) was 2 mm. When the side sealing pads (1.3 mm, when pressure squeezed; 0.3 mm) and the other parts were tightly assembled, the actual internal flow thickness was 0.8 mm.

The FHP system used in this experimental study was manufactured with copper at the full-size of 170 × 120 × 5.8 (mm). The total thickness of the flat heat pipe depends on the type of internal wicks, and the wick size of the experimental system was 150 × 100 (mm). Figure 2(c) shows a photo of the metal fiber wick taken by scanning electron microscope (SEM). According to the tests, the measured pore size (*r*), porosity (ε) and permeability (α) are SUS (*r* = 15 μm, ε=0.9, $\alpha=1.0066\times10^{-10}$ m^2) and copper (*r*= 58 μm, ε=0.78, $\alpha=1.9793\times10^{-10}$ m^2).

The heater was made of 150 W power cartridge heaters, and the total heat supplying area was 1250 mm^2. The amount of power supplied to the heater was calculated by measuring the voltage and current supplied by the power transformer (UP 3050). To prevent heat loss, all sides of the heater surface, except the sides attached to the evaporation section, were insulated. The contact space between the heater and evaporator were filled with a thermal contact pad (*k* = 2 W/m·K), and the condenser section was cooled by the 80 mm axial fan. As shown in Figure 2(b), to measure the temperature of the system, nine thermocouples at the top and bottom of the heat pipe and one thermocouple (K-Type) on the heater surface were installed at 19 points. To measure the isotherm distribution of the instantaneous temperature, an infrared thermometer was used to observe and record.

From 5 to 20 W, the amount of heat supplied was varied in 5 W

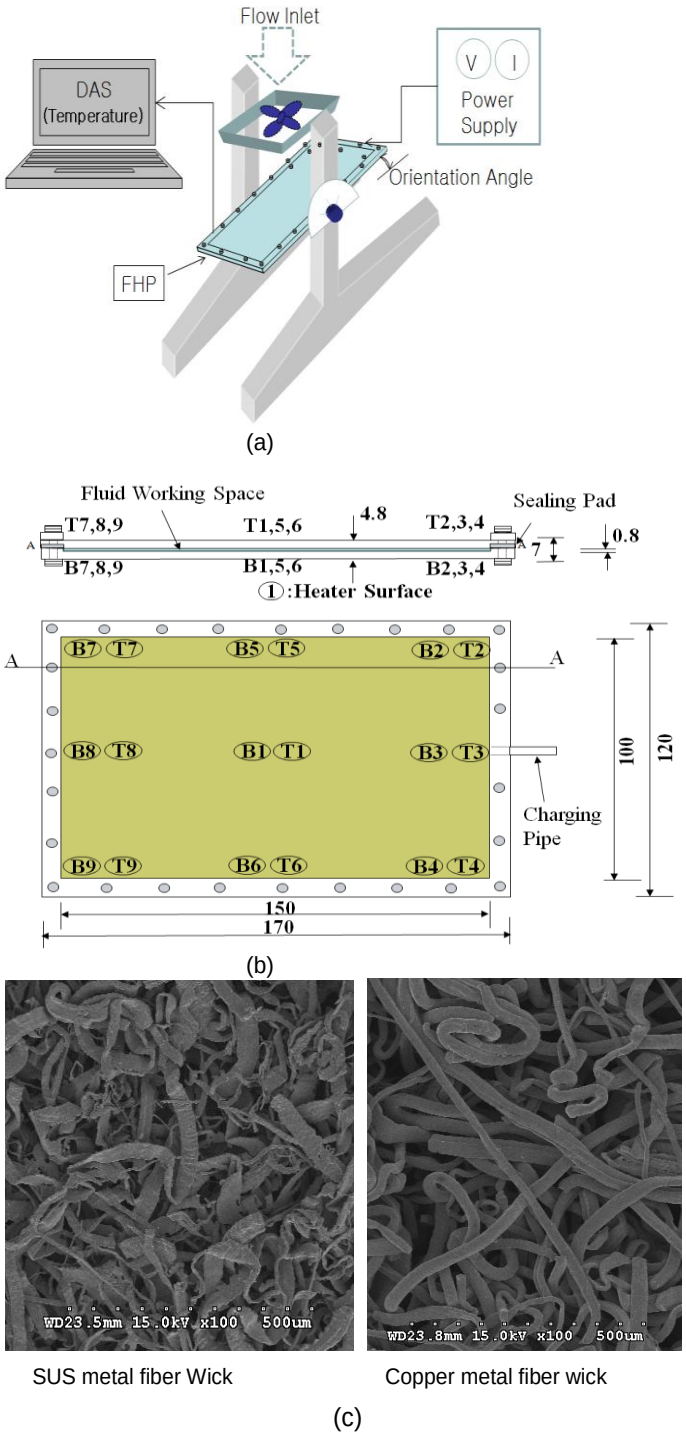

Figure 2. Schematic design and wick structure of flat plate heat pipe; (a) Experimental setup (b) FHP schematic design (c) wick structures.

steps, and both natural and forced-convective experiments were conducted. In addition to the horizontal mode, experimental data with a 45° and 90° (vertical mode) orientation in 20 W were analyzed. A fan was installed 100 mm above the condensation section.

To find the most suitable working fluid for the system, refrigerants such as ethanol, water, acetone and nanofluids were tried under various conditions. Theoretically, any kind of fluid could be used as the working fluid, but water was the best choice. Water has a high latent heat thermal property, permits the transmission of heat more than all other working fluids, is cheap, easily available, and is non-combustible. In the present study, the TiO_2-nanofluids used were particle suspended fluids with TiO_2 nanoparticles ranging in size from 27 to 56 nm with water as the base fluid, and was supplied by NanoANP Co, Korea. The nanofluids were mixed in the TiO_2-nanofluid and water, and the mixture was sonicated for 16 to 20 h to get a reliable mix in an ultrasonic bath with a specified volume concentration (DaeRyun Science Inc., Korea).

An important constraint in the operation of a flat heat pipe is the effect of the amount of working fluid charged in the heat pipe. Imura et al. (1993) suggested a useful estimation for V^+. In the present study, the charged amount of working fluid was estimated as the ratio V^+, which was defined as the ratio between the volume of charged amount and the total inner volume of the heat pipe. The optimum amount was investigated experimentally. With the resulting information, one can determine the optimum amount of a given working fluid, so a series of experiments were carried out to determine the optimum V^+. In the preliminary test, V^+ = 0.5~0.6 performed the best, so various investigations were conducted with this ratio.

Data acquisition device MX100 Yokogawa was used, and the working fluid was injected into the device after the inner pressure reached to 0.01 torr in vacuum. As shown in Figure 3, various experiments with eight wick types were performed to find an optimum wick. Also the experimental combinations between wick structures and working fluids were specified in Table 1.

Before the start of an experiment, the FHP was thoroughly cleaned and washed with ethanol and then with distilled water. Great care was taken to remove all the air and other non-condensable gases from the charging system. The power to the evaporator section was carefully increased in increments to the desired heat flux. It took approximately 1 h to reach steady state.

The air flow velocity and air temperature were measured with the thermo-anemometer. Once the system was stable, all the data were recorded. After each series of tests for a given working fluid, the FHP was again thoroughly cleaned, washed, vacuum dried and checked for leaks. After the system was evacuated, a known amount of a new test working fluid was charged into the test tube and the subsequent series of tests was performed using the same procedures.

The heat loss through the system was negligible because the heating and the evaporator sections were well insulated. The uncertainties involved in the data reduction for the heat transfer performance and thermal resistance were generally due to the inaccuracy of the temperature and the power measurements read from the instruments. Despite the fact that the readings of the power and the temperatures were recorded with a regulated DC power supply (±0.03% for voltage and current) and MX-100 Data acquisition system (±0.05% for temperature). The uncertainty for thermal resistance based on supplied heat was ±0.28%.

RESULTS AND DISCUSSION

In order to evaluate the performance of heat pipes, the thermal resistance of the heat pipes was compared with various wick structures. The FHP with various wick structures was tested with a variety of working fluids such as water, acetone, ethanol and the nanofluids. Figure 4 shows the performance of the flat heat pipe developed in this study in terms of thermal resistance on Q.

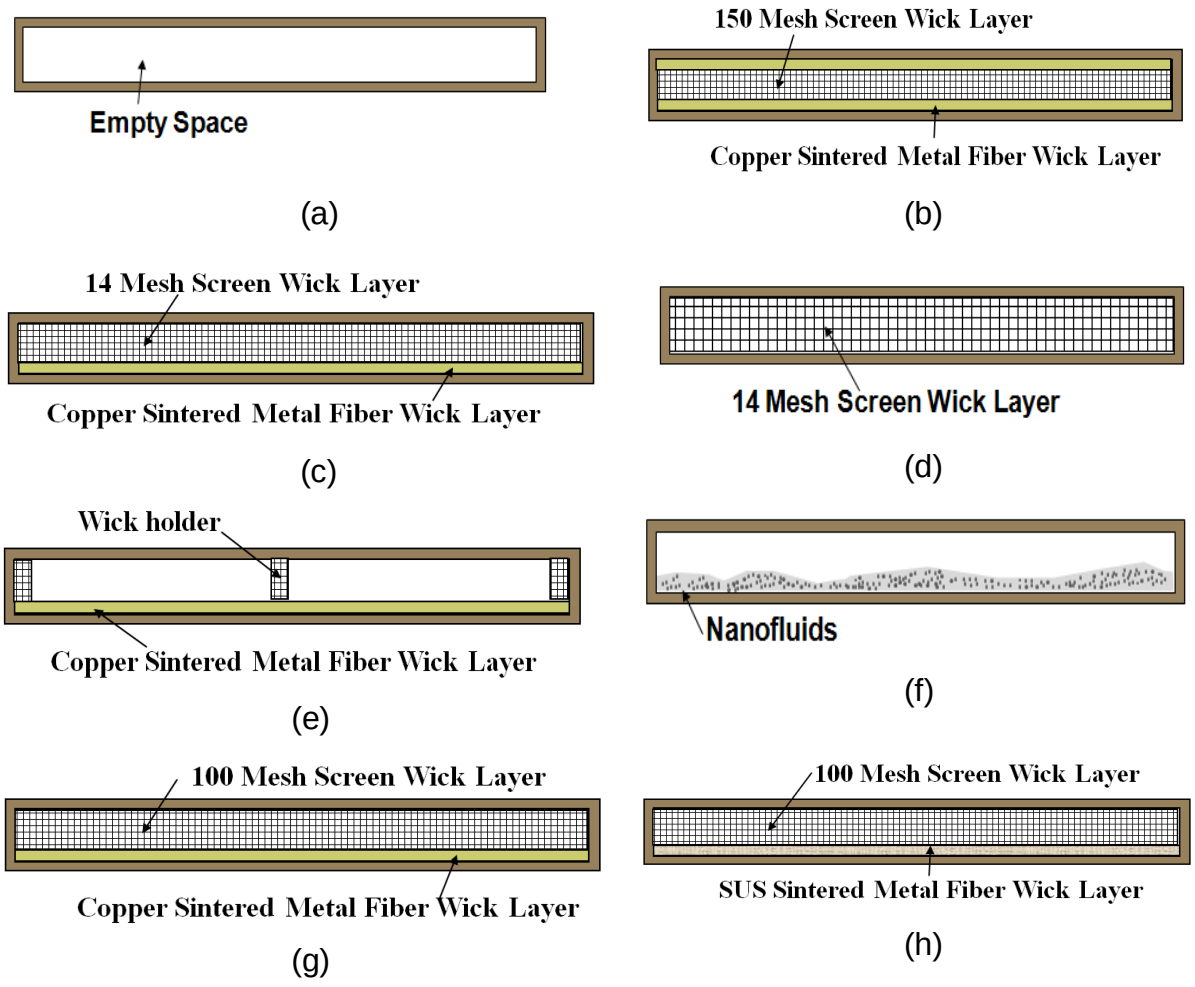

Figure 3. Wick configurations; (a) Flat thermosyphon (b) wick 1 (c) wick 2 (d) wick 3 (e) wick 4 (f) nanofluid system (g) wick 5 (h) wick 6.

Table 1. Combinations of wick and working fluid.

Wick and working fluid combinations	Wick type	Working fluid
1	(a)	Water
2	(b)	Water
3	(d)	Water
4	(c)	Water
5	(e)	Water
6	(a)	Water
7	(a)	Acetone
8	(a)	Ethanol
9	(f)	0.05% TiO_2-Water
10	(f)	0.1% TiO_2-Water
11	(g)	Water
12	(h)	Water
13	(g)	Acetone
14	(h)	Acetone
15	(g)	Ethanol
16	(h)	Ethanol

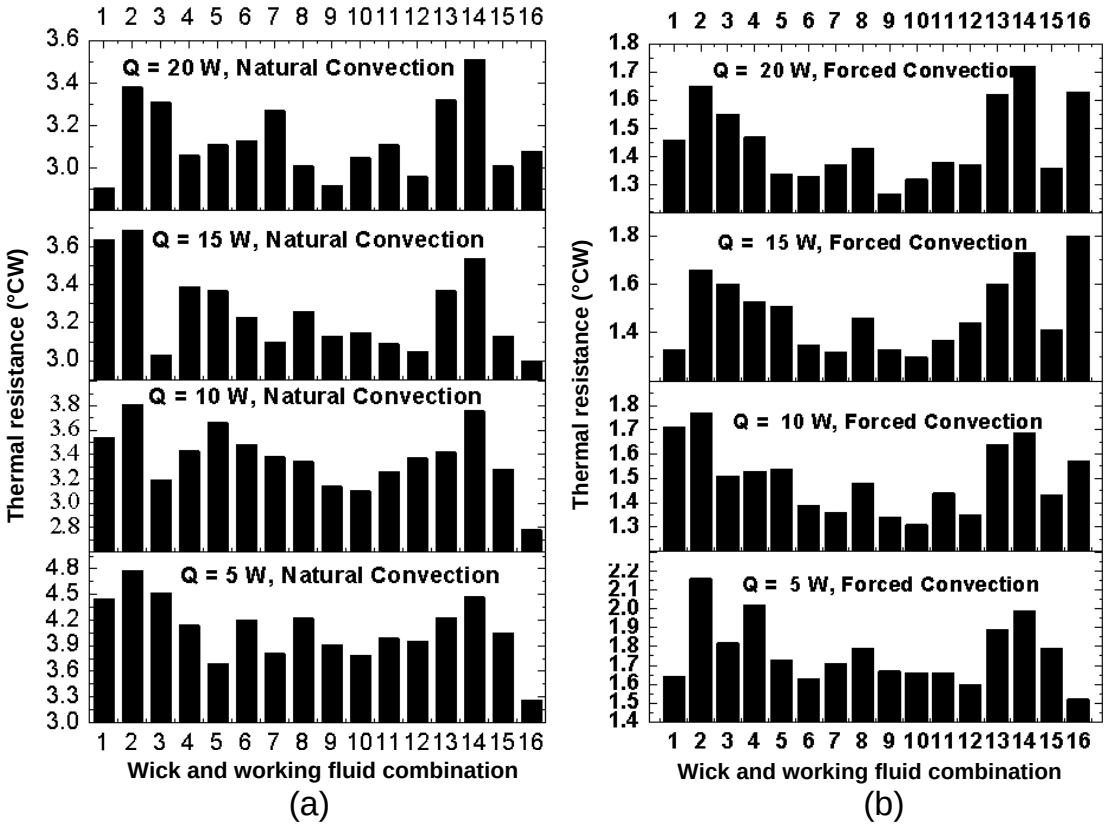

Figure 4. Effect of different types of flat heat pipe; (a) Heat transfer performance with different working fluids, natural convection (b) effect of working fluids, effect of thermal resistance, forced convection.

Figure 4(a) and (b) shows the effect of various wick structures and working fluids for natural and forced convection modes. As shown in Figure 4(a), with a natural convection mode, the best cooling performance was obtained from wick 6 with ethanol in the range of 5~15 W. In the 20 W of heat flux, the flat thermosyphon exhibited the lowest thermal resistance. Nanofluidic FHP had low thermal resistance compared to other combinations, but mainly the thermosyphhonic system [Wick (a), (e), and (f)] has better heat transfer performance. As shown in Figure 4(b) for forced convection, with the exception of 20 W, systems using 0.1% - TiO_2-nanofluid showed the most suitable heat transfer performance. This is due to the improvement of heat transfer performance caused by an increase in thermal conductivity. In addition, somewhat better enhancement of heat transfer performance was observed with an increase in nanofluid concentrations, and various thermal performance evaluations were performed based on it. The worst FHP performance was obtained from (c) wick 2 with water as the working fluid. This implies that the complex wick structure in micro flat space is unsuitable. From Figure 4(a) and (b), it could be considered that the thermosyphonic FHP heat spreader showed better performance in both natural and forced convection mode. But the TiO_2-nanofluidic system with thermosyphonic structure showed slightly lower thermal resistance compared to other working fluids.

In Figure 5, using the temperature difference between the heater temperature and ambient temperature according to changes in the orientation of the FHP system, the thermal performance was evaluated. The experiments were carried out using pure water, acetone and ethanol as working fluids for different wick structures. As shown in Figure 5, depending on the orientation, there did not seem to be a large difference in the heat transfer performance, so it seems that the current flat heat pipe was not greatly affected by the orientation. The results with (a) ethanol (V^+ = 0.6) showed a slight orientation effect; however, the others with ethanol showed a similar trend with other wicks and working fluid combinations.

Because the FHP used in this research was air cooled in the forced convection mode, the effect of inlet air flow velocity in the condenser was investigated, as shown in Figure 6. Figure 6 shows the effect of the air velocity in the condenser section on the overall temperature difference, $\Delta T_{h\text{-}c}$ of the systems. The velocity of air on the condenser section is a factor which affects the heat transfer capability of the system. It was seen that the total thermal resistance was reduced because of the increased convective heat transfer on the condenser section. However, Figure 6 also shows that an increase

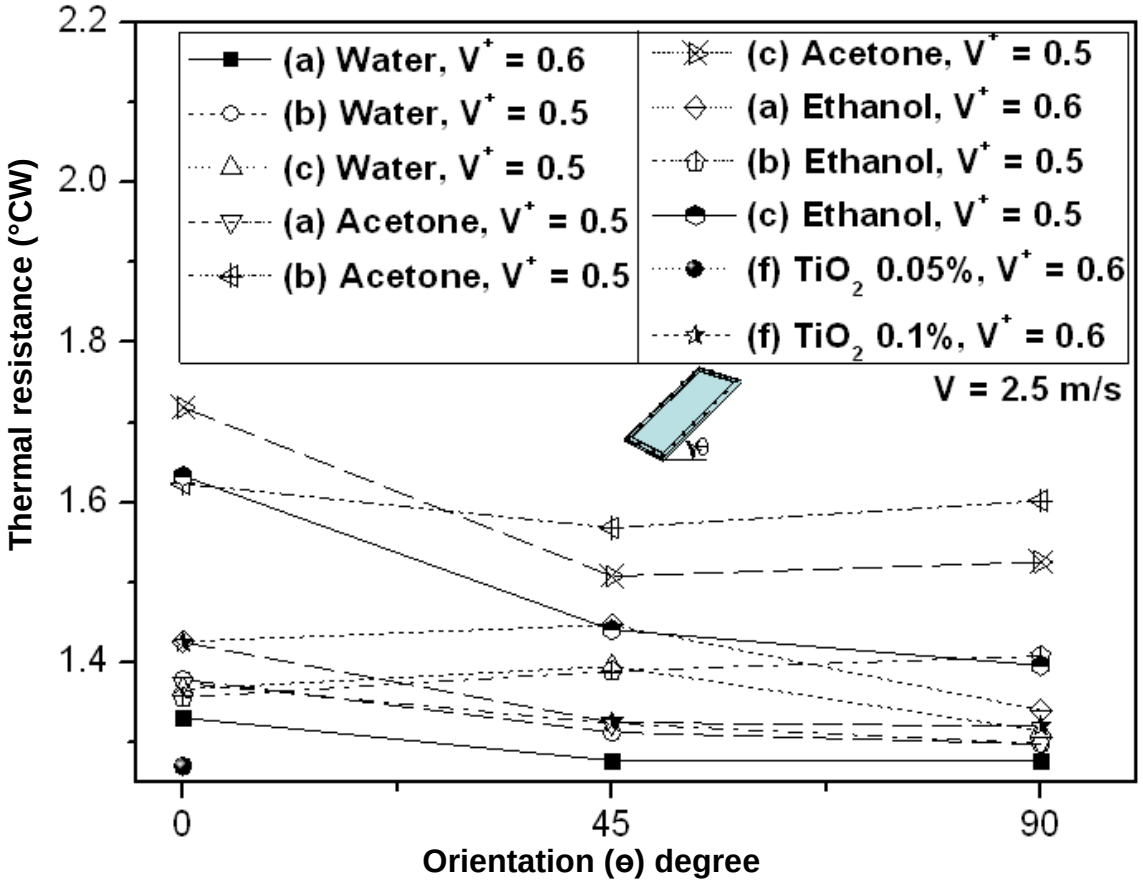

Figure 5. Effect of orientation (Q = 20 W, forced convection).

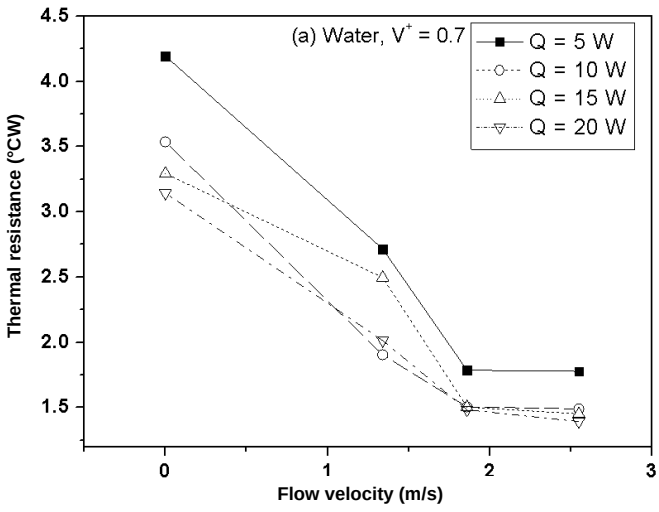

Figure 6. Heat transfer performance of flat plate heat pipe with air flow velocity.

in the air velocity greater than 1.9 m/s did not significantly increase the overall heat transfer capacity of the assembly. The reason for this phenomenon is that the air flow velocity on the condenser section has little effect on the forced convection heat transfer coefficient (h_{cond}), once the air velocity is greater than 1.9 m/s. Even though the heat transfer capacities of the working fluids were different, a similar tendency was observed.

As shown in Figure 7, when the temperature distribution of FHP was 20 W input power, the system showed the most outstanding performance. Also, when using the 0.1% - TiO_2-nanofluid, the difference of the spreading temperature distribution was 5°C. It is a more outstanding performance than the 16°C difference that occurred when distilled water was used.

As shown in Figure 8 and 9, the temperature distribution with sintered copper wick and water as the working fluid had comparable results in the case of thermosyphon and FHP with copper fiber wick structure with two heat inputs (5 W for Figure 8, and 20 W for Figure 9). As shown in Figure 8 and 9, the simulation result for the one-dimensional thermal resistance network model was recalculated and compared to the two-dimensional isothermal temperature distribution in FHP, and the entire temperature distribution due to the heat spreading nearly matched the temperature distribution simulated with modified Song et al.'s (1994) equation. Through continuous comparison between the experiment and simulation, the experimental constant value of

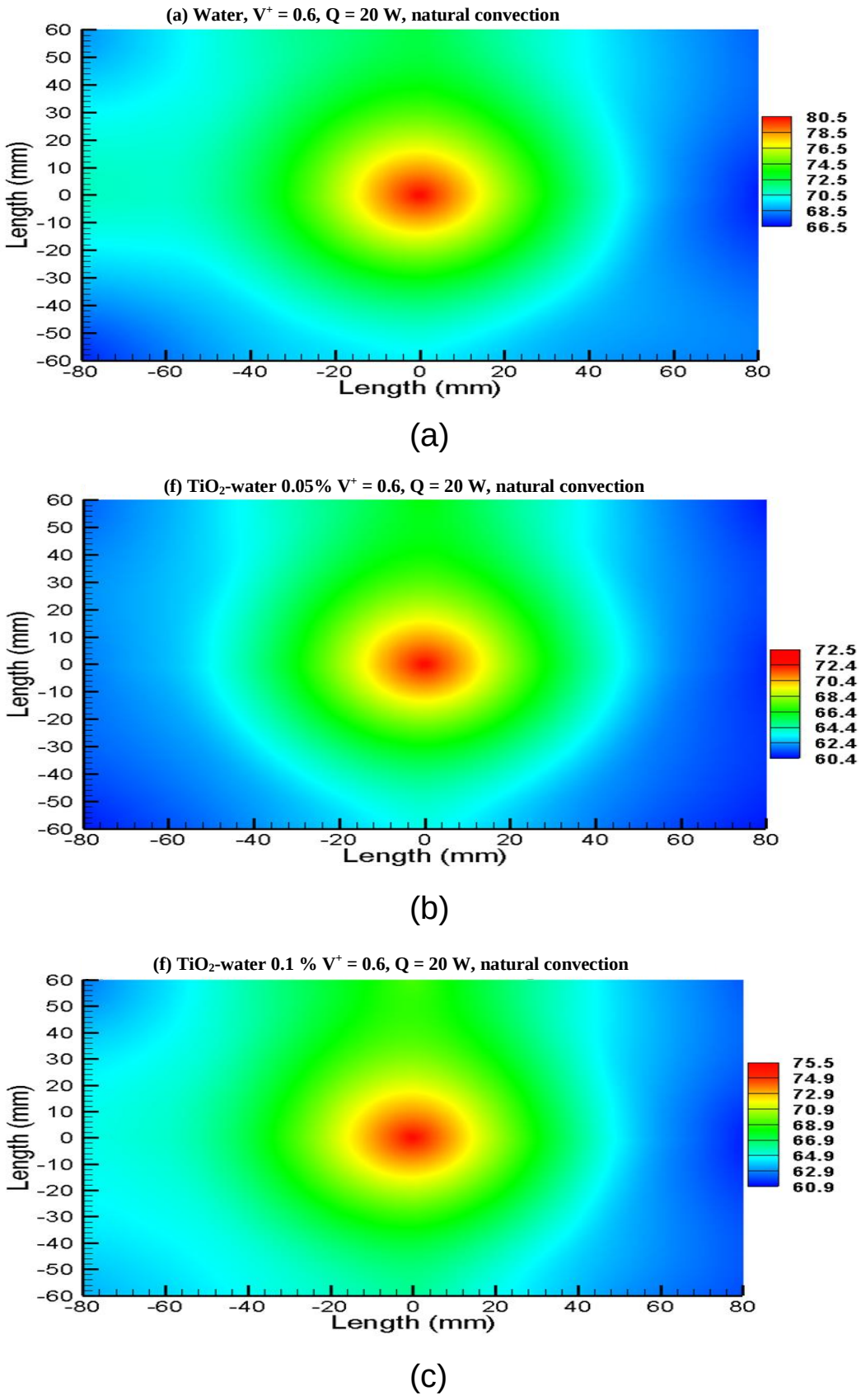

Figure 7. Temperature profile in top surface with TiO_2-nanofluid; (a) Water (b) nanofluid, TiO_2 –water, 0.05% (c) nanofluid, TiO_2 –water, 0.1%.

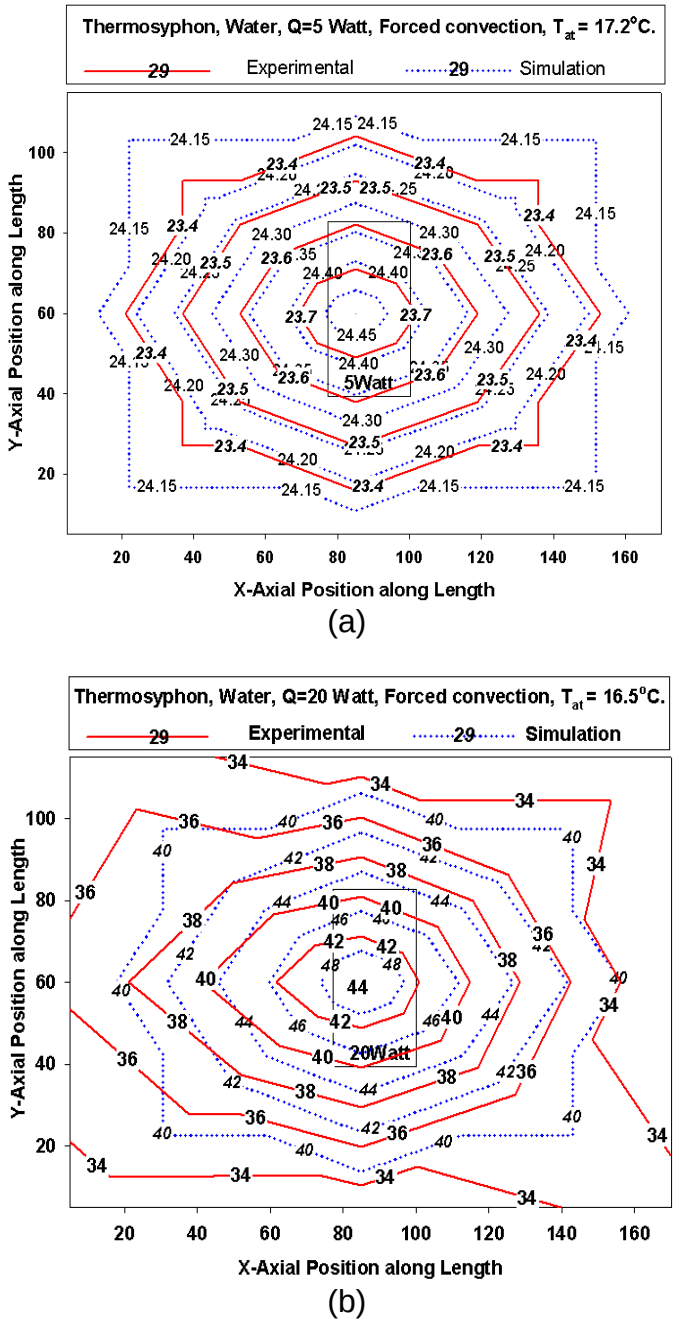

Figure 8. Temperature distribution, comparison between experiments and simulation, flat Thermosyphon; (a) Q = 5 W (b) Q = 20 W.

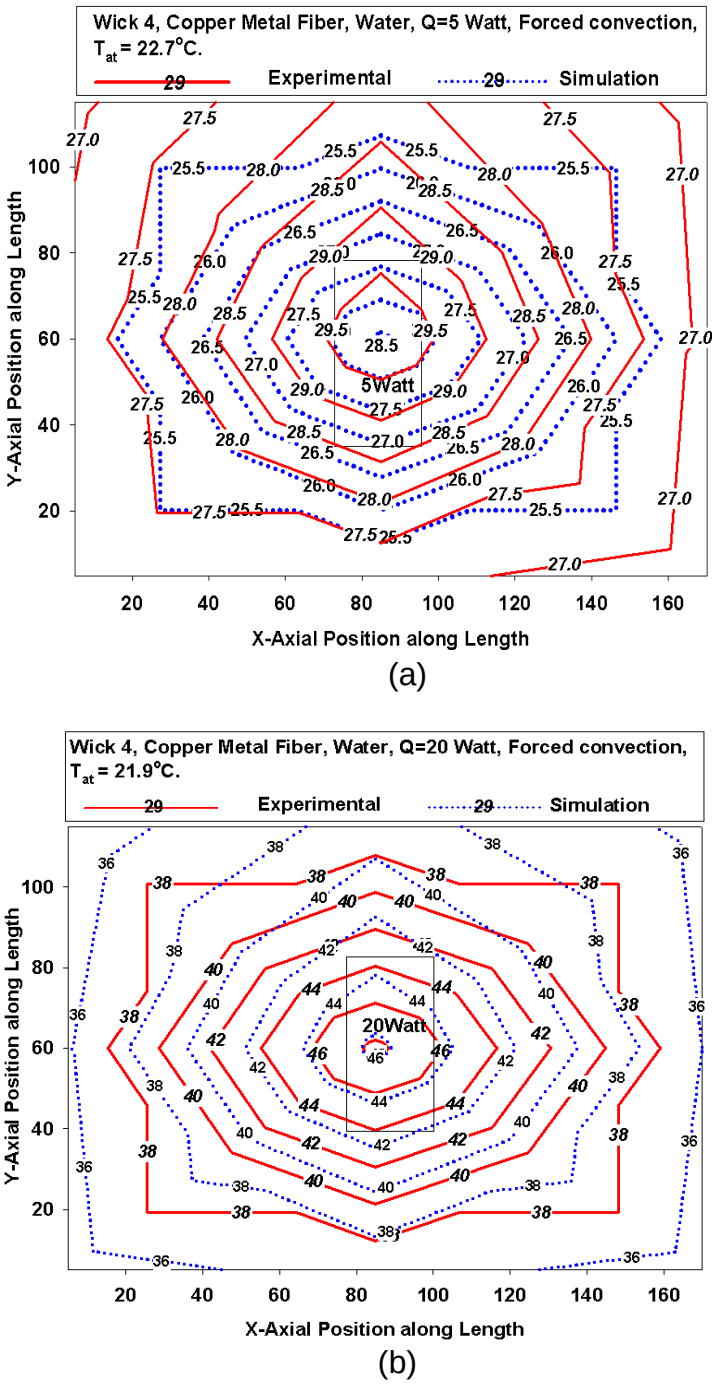

Figure 9. Temperature distribution, comparison between experiments and simulation, wick 4 with copper metal fiber (a) Q = 5 W (b) Q = 20 W.

spreading thermal resistance *C* value in Equation 5 was derived to be 10.0.

Conclusion

The purpose of this study was to evaluate the performance of flat heat pipe heat spreader and increase the thermal diffusion and cooling efficiency, as well as, determines the effect of various wick structures and working fluids on heat spreading performance. The performance of the FHP was evaluated by applying various wicks. Experiments to evaluate the heat transfer performance were carried out up to the maximum 20 W heat input. A high heat transfer and cooling performance

was seen when using 0.1% TiO_2-nanofluid with thermosyphon structure without any complexity, and the working fluid inside the heat pipe with the best performance was observed when the amount of filling was 50 to 60%. In addition, when examining the effects of changing the flow rate of the cooling fan, it was observed that the optimal point of the air flow rate could increase the heat transfer performance of the flat heat pipe heat spreader.

ACKNOWLEDGEMENT

This work was supported by the research grant of the Chungbuk National University in 2011.

Nomenclature: A, Area [m^2]; ***A*$_b$,** Heat spreader base area [m^2]; ***A*$_s$,** Heat source area [m^2]; ***Bi*,** Effective Biot Number, $Bi = (h_{eff}\sqrt{A_b/\pi})/k$ in Equation 4; ***D*,** Diameter [m]; ***g*,** acceleration of gravity [m/s^2]; ***h*,** heat transfer coefficient [$W/m^2°C$]; ***k*,** thermal conductivity [W/m°C]; ***L*,** length [m]; ***Nu*,** Nusselt number; ***P*,** pressure [Pa]; ***Pr*,** Prandtl number; ***Q*,** heat transfer rate [W]; ***R*,** resistance [°C/W]; ***Re*,** Reynolds number; ***T*,** temperature [°C]; ***t*,** thickness [m]; **V+,** filling ration of working fluid [(charged amount volume)/(total inner volume of the heat pipe)].

Greek symbol: *α*, Permeability [m^2]; ***δ*,** thickness [m]; ***ε*,** porosity, dimensionless contact radius, $\varepsilon = \sqrt{A_s/\pi}\,/\sqrt{A_b/\pi}$ in related in Equation 5; ***λ*,** eigenvalue, $\lambda = \pi + 1/\varepsilon\sqrt{\pi}$ in Equation 4; ***ψ*,** dimensionless constriction resistance [°C/W]; τ **,** $\tau = t/A_b$ in Equation 5; ***ρ*,** density [kg/s]; *μ*, viscosity [kg/m·s].

Subscripts: at, Surrounding air; **c,** condenser; case, top or bottom heat pipe case; **cc,** condenser case; **cr,** vapor core radius; **e,** evaporator; **ec,** evaporator case; **eff,** effective; **e,p,** evaporator vapor pass; **v,e,** vapor in evaporator section; **v,c,** vapor in condenser; **f,** fluid only; **fg,** fluid-gas; **g,** gas only; **l,** liquid; **rh,** rectangular heater; **s,** heat source; **sr,** spreading resistance; **tp,** thermal pad; **v,** vapor.

REFERENCES

Avenas Y, Ivanova M, Popova N, Schaeffer C, Schanen JL, Bricard A (2002). Thermal analysis of thermal spreaders used in power electronics cooling. Ind. Appl. Conf., 37th IAS Annu. Meet., 1: 216–221.

Chi SW (1976). Heat Pipe Theory and Practice a Sourcebook, Washington : Hemisphere Pub. Corp.

Go JS, Kim KC (2004). An Isothermal Temperature Source with a Large Surface Area using the Metal-Etched Micro wick-Inserted Vapor Chamber Heat Spreader. J. Mech. Sci. Technol., 18: 681~688.

Holman JP (1996). Heat Transfer. 8th ed., McGraw-Hill Book Company, New York.

Hui P, Tan HS (1994). Temperature distribution in a heat dissipation system using a cylindrical diamond heat spreader on a copper heat sink. J. Appl. Phys., 75: 748-757.

Imura H, Sasaguchi K, Kozai H (1993). Critical Heat Flux in a Two Phase Closed Thermosyphon. Int. J. Heat Transf., 26(8): 1181-1188.

Kalahasti S, Yogendra KJ (2002). Performance Characterization of a Novel Flat Plate Micro Heat Pipe spreader. IEEE Trans. Compon. Packaging Technol., 25: 554-560.

Kang SW and Tsai SH (2004). Metallic micro heat pipe heat spreader fabrication. Appl. Therm. Eng., 24: 299-309.

Kim HT, Lee YD (2003). A Study on the Heat Spreading Characteristic of a Heat Spreader. SAREK Summer Conference Pro.,. 1172-1177.

Kwark SM (2005). The thermal characteristics of liquid-heat-spreader. MS Thesis, University of Texas, Alington.

Lee JS, Kim TG, Park TS, Kim CS, Park CH (2002). An Analytic Study on Laminar Film Condensation along the Interior Surface of a Cave-Shaped Cavity of a Flat Plate Heat Pipe. KSME Int. J., 16: 966-974.

Lee KW, Park KW, Rhi SH, Yoo SY (2002). Heat Pipe Heat Sink Development for Electronics Cooling. SAREK J., 14: 664-670.

Oh PK, Byun KS (2001). A Study on characteristics on Flat type miniature heat pipe. SAREK Winter Conf. Proc., pp. 339-344.

Savchenkov GA, Gorbis ZR (1976). Boiling Heat Transfer in Low Temperature Evaporating Thermosiphons. Proc. 5th All-Union Conf. Heat Mass Transf., 13: 87-91.

Song SH, Lee S (1994) Closed-Form Equation for Thermal Constriction/Spreading Resistances with Variable Resistance Boundary Condition. IEPS Conf., pp. 111-121.

Thomas W, Goodson KE, Santiago JG, Wang E, Koo JM , Linan J, Pop E, Sinha S, Lian Z, Fogg D, Shuhuai Y, Flynn R, Chang CH, Hidrovo CH (2006). Advanced Cooling Technologies For Microprocessors. Int. J. High Speed Electron. Syst., 16 (1): 301-313.

Tsai CY, Chien HT, Ding PP, Chan P, Luh TY, Chen PH (2004) Effect of structural character of gold nanoparticles in nanofluid on heat pipe thermal performance. Mater. Lett., 58: 1461–1465.

Wang JC (2011). Thermal investigations on LED vapor chamber-based plates. Int. Commun. Heat Mass Transf., 38: 1206–1212.

Wong SC, Lin YC, Liou JH (2012). Visualization and evaporator resistance measurement in heat pipes charged with water, methanol or acetone. Int. J. Therm. Sci. 52: 154-160.

Yasushi K, Hideaki I, Masataka M, Yuji S, Shuichi T (2006). Numerical analysis and experimental verification on thermal fluid phenomena in a vapor chamber. Appl. Therm. Eng., 26: 1669–1676.